



HAL
open science

Borna Disease Virus Phosphoprotein Modulates Epigenetic Signaling in Neurons To Control Viral Replication

Emilie Bonnaud, Marion Szelechowski, Alexandre Betourne, Charlotte Foret,
Anne Thouard, Daniel Gonzalez-Dunia, Cécile Malnou

► **To cite this version:**

Emilie Bonnaud, Marion Szelechowski, Alexandre Betourne, Charlotte Foret, Anne Thouard, et al.. Borna Disease Virus Phosphoprotein Modulates Epigenetic Signaling in Neurons To Control Viral Replication. *Journal of Virology*, 2015, 89 (11), pp.5996-6008. 10.1128/JVI.00454-15 . hal-02402637

HAL Id: hal-02402637

<https://hal.science/hal-02402637>

Submitted on 10 Nov 2021

HAL is a multi-disciplinary open access archive for the deposit and dissemination of scientific research documents, whether they are published or not. The documents may come from teaching and research institutions in France or abroad, or from public or private research centers.

L'archive ouverte pluridisciplinaire **HAL**, est destinée au dépôt et à la diffusion de documents scientifiques de niveau recherche, publiés ou non, émanant des établissements d'enseignement et de recherche français ou étrangers, des laboratoires publics ou privés.

1
2
3
4
5
6
7
8
9
10
11
12
13
14
15
16
17
18
19
20
21
22
23

Borna disease virus phosphoprotein modulates epigenetic signaling in neurons to control viral replication

Emilie M. Bonnaud^{1,2,3,#}, Marion Szelechowski^{1,2,3,#}, Alexandre Bétourné^{1,2,3}, Charlotte Foret^{1,2,3}, Anne Thouard^{1,2,3}, Daniel Gonzalez-Dunia^{1,2,3} and Cécile E. Malnou^{1,2,3,*}

¹INSERM UMR 1043, Centre de Physiopathologie de Toulouse Purpan (CPTP), Toulouse, F-31300, France; ²CNRS UMR 5282, Toulouse, F-31300, France; ³Université Toulouse III Paul Sabatier, Toulouse, F-31300, France.

[#]Contributed equally and should be considered joint first authors

^{*}To whom correspondence should be addressed. Email: cecile.malnou@inserm.fr

Running title: BDV phosphoprotein modulates neuronal epigenetics

Abstract word count: 243

Importance word count: 116

24

25 **Abstract**

26

27 Understanding the modalities of interaction of neurotropic viruses with their target cells
28 represents a major challenge that may improve our knowledge of many human neurological
29 disorders for which viral origin is suspected. Borna disease virus (BDV) represents an ideal
30 model to analyze the molecular mechanisms of viral persistence in neurons and its
31 consequences for neuronal homeostasis. It is now established that BDV ensures its long-
32 term maintenance in infected cells through a stable interaction of viral components with the
33 host cell chromatin, in particular with core histones. This has led to our hypothesis that such
34 an interaction may trigger epigenetic changes in the host cell. Here, we focused on histone
35 acetylation, which play key roles in epigenetic regulation of gene expression, notably for
36 neurons. We performed a comparative analysis of histone acetylation patterns of neurons
37 infected or not by BDV, which revealed that infection decreases histone acetylation on
38 selected lysine residues. We showed that the BDV phosphoprotein (P) is responsible for
39 these perturbations, even when expressed alone independently of the viral context, and that
40 this action depends on its phosphorylation by protein kinase C. We also demonstrated that
41 BDV P inhibits cellular histone acetyl transferase activities. Finally, by pharmacologically
42 manipulating cellular acetylation levels, we observed that inhibiting cellular acetyl
43 transferases reduces viral replication in cell culture. Our findings reveal that manipulation of
44 cellular epigenetics by BDV could be a mean to modulate viral replication and thus illustrate
45 a fascinating example of virus/host cell interaction.

46

47

48

49 **Importance**

50

51 Persistent DNA viruses often subvert the mechanisms that regulate cellular chromatin
52 dynamics, thereby benefitting from the resulting epigenetic changes to create a favorable
53 milieu for their latent/persistent states. Here, we reasoned that Borna Disease Virus (BDV),
54 the only RNA virus known to durably persist in the nucleus of infected cells, notably
55 neurons, might employ a similar mechanism. In this study, we uncover a novel modality of
56 virus/cell interaction in which BDV phosphoprotein inhibits cellular histone acetylation by
57 interfering with histone acetyl transferase activities. Manipulation of cellular histone
58 acetylation is accompanied by a modulation of viral replication, revealing the perfect
59 adaptation of this "ancient" virus to its host that may favor neuronal persistence and limit
60 cellular damage.

61

62

63 **Introduction**

64 Long-term persistence in the host cell is a real challenge for viruses, since it requires a
65 tight control of viral replication in order to limit cytopathic effects. This is notably the case
66 for viruses infecting cells with poor renewal capacities, such as neurons. Thus, neurotropic
67 viruses provide a unique opportunity to decipher the molecular mechanisms underlying
68 virus-cell interactions during persistence. Moreover, a better understanding of the
69 physiological consequences of viral persistence in the central nervous system (CNS) may
70 also help to clarify some unknown aspects of neuronal physiology, in normal and
71 pathological conditions (1, 2).

72 Borna disease virus (BDV) represents an ideal paradigm for investigating the modalities
73 of persistence of a non-cytolytic virus in the CNS. BDV exhibits a selective tropism for
74 neurons of the limbic system, in particular the cortex and hippocampus, two structures that
75 govern many cognitive and behavioral functions (3). Although BDV is highly neurotropic, it
76 can also replicate in other cells of the CNS, as well as in many established cell lines *in vitro*.
77 BDV infects a wide variety of mammals, leading to a large spectrum of neurological
78 disorders, ranging from acute encephalitis to behavioral alterations without inflammation (4,
79 5). Despite this wide host range, there is still controversy regarding whether BDV can infect
80 humans and be associated with neurological diseases (2). The recent detection of
81 endogenized BDV-like sequences in a wide array of species, including primates, has
82 however established that ancient bornaviruses actually infected our ancestors nearly 40
83 million years ago, thus revealing the long co-evolution between bornaviruses and animal
84 species (6).

85 BDV is an enveloped virus, with a non-segmented, negative strand RNA genome of 8.9
86 kb, the smallest of the *Mononegavirales* order (7). Its compact genome encodes six proteins,
87 namely, the nucleoprotein (N), phosphoprotein (P), protein X, matrix protein (M),
88 glycoprotein (G), and polymerase (L). Whereas M and G are involved in particle formation,
89 P, N, and L are components of the ribonucleoprotein complex (RNP). One striking feature of
90 BDV infection resides in the location of RNP into the nucleus, where viral transcriptions and
91 replication take place (1). This is an exception for vertebrate RNA viruses, which usually
92 replicate in the cytoplasm of infected cells. The only other family of RNA viruses that

93 replicates in the nucleus, the *Orthomyxoviridae*, are cytolitic (3). Hence, BDV is the only
94 RNA virus that durably persists in the nucleus of infected cells.

95 To achieve this efficient intra-nuclear persistence, BDV closely associates with
96 chromatin and forms viral factories, designated as vSPOTs (viral SPeckles Of Transcripts),
97 which contain all viral components necessary for viral transcriptions. It was shown that
98 vSPOTs interact in a dynamic manner with host chromosomes, using High Mobility protein
99 Group B-1 (HMGB-1) as a scaffold protein between RNP and chromatin (1, 8). Based on
100 these findings, it was tempting to hypothesize that BDV may modify the host cell chromatin,
101 or interact with factors controlling chromatin dynamics. Moreover, in a previous proteomic
102 analysis using primary neuronal culture protein extracts, we observed that acetylation of
103 histone H2B was changed upon infection, suggesting that epigenetic signaling could indeed
104 be affected by BDV (9).

105 Amongst the multiple modes of virus-mediated hijacking of host cell functions,
106 manipulation of epigenetic signaling appears particularly well suited for persistent viruses,
107 especially for DNA viruses. This allows them to benefit from epigenetic changes they
108 induce in the nucleus of target cells, thereby producing a favorable environment for their
109 latent/persistent states or for reactivation (10-13). This has been well described for
110 herpesviruses, such as Kaposi's sarcoma-associated herpesvirus, for which the latency-
111 associated nuclear antigen has been shown to interact with host chromatin modifiers and
112 induce epigenetic reprogramming (14, 15). Such a scenario appeared however less likely for
113 RNA viruses. The long lasting nuclear persistence of BDV, together with its close
114 association to chromatin, led us to hypothesize that, similarly to large DNA viruses, BDV
115 infection could be accompanied by virus-mediated changes in the host cell epigenome.

116 As histone acetylation is a crucial modification allowing a fine control of neuronal gene
117 expression and is often perturbed in numerous neurological pathologies (16, 17), we sought
118 to analyze the impact of BDV infection on epigenetic signaling, with a particular focus on
119 histone acetylation patterns. Using both primary neuronal cultures and persistently infected
120 cell lines, we demonstrate that BDV infection leads to a decrease of histone acetylation
121 levels, restricted to specific H2B and H4 lysine residues. We also identify the BDV P as the
122 viral determinant responsible for this inhibition and show that it needs to be phosphorylated
123 by the protein kinase C (PKC) to exert this effect. Finally, we show that decreased histone

124 acetylation is due to inhibition of cellular histone acetyl transferases (HATs) and that
125 pharmacological manipulation of cellular acetylation modulates viral replication. This
126 suggests that inhibition of histone acetylation may serve to control viral replication during
127 persistence.

128

129 **Materials and methods**

130

131 **Ethics statement.** Animal handling and care for the preparation of primary neuronal
132 cultures from rat embryos was performed in accordance with the European Union Council
133 Directive 86/609/EEC and experiments were performed following the French national chart
134 for ethics of animal experiments (articles R 214- 87 to 90 of the “Code rural”). Our protocol
135 received approval from the local committee on the ethics of animal experiments (permit
136 number: 04-U1043-DG-06). Pregnant rats were deeply anesthetized with CO₂ before
137 euthanasia to minimize suffering.

138

139 **Primary neuronal cultures, virus infection and plasmid transfection.** Primary cortical
140 neurons were prepared from Sprague-Dawley rat embryos at gestational day 17 by the
141 papain dissociation method as described previously (18). At the end of the procedure,
142 neurons were either directly plated on variable supports (glass coverslips or culture plates)
143 depending on the experiments, or used for plasmid transfection before plating. Before
144 seeding, supports were coated with 500 µg/ml poly-ornithine (Sigma), followed by 5 µg/ml
145 laminin (Roche). Neurons were maintained in Neurobasal medium (Invitrogen)
146 supplemented with 100 µg/ml penicillin/streptomycin, 0.5 mM glutamine and 2 % B-27
147 supplement (Invitrogen). Half of each culture was infected 4 h after plating with cell-free
148 BDV. Cell-released virus stocks were prepared as described using Vero cells persistently
149 infected by wild-type BDV (Giessen strain He/80) or different recombinant BDV (rBDV)
150 (19). By 14 days post-infection, the efficacy of viral spread into the culture (which routinely
151 attained >95 %) was systematically assessed by indirect immunofluorescence for the
152 detection of BDV antigens.

153 To achieve efficient expression of isolated BDV proteins, neurons were transfected
154 using Amaxa technology and the rat neuron nucleofector kit (Lonza) following the
155 manufacturer instructions (5.10⁶ neurons with 3 µg of plasmid DNA, using the G-13
156 program), allowing routine transfection efficiencies of at least 75 % for primary neurons.

157 Neurons were plated for 14 days, a time at which transfection efficiency was systematically
158 verified by indirect immunofluorescence before proceeding to histone preparation. Plasmids
159 used for transfection contained genes encoding BDV N or BDV P proteins under the control
160 of the CMV early enhancer/chicken β actin (CAG) promoter, or an empty vector as a control.
161 In addition, two plasmids encoding different mutants of BDV P were used, one in which the
162 glutamate residue in position 84 was replaced by an asparagine (P_{E84N}) to abolish interaction
163 with HMGB1 (19), and another for which serine residues at positions 26 and 28 were
164 replaced by alanine residues (P_{AA}) to mutate the PKC phosphorylation site of P (19). All
165 plasmids were kind gifts from Pr. Schwemmler. Plasmid maps are available on request.

166

167 **Cell lines, production of lentiviral vectors and transduction experiments.** Vero and
168 HEK-293T cells were obtained from the American Type Culture Collection. We also used
169 Vero cells persistently infected with either wild-type BDV (Giessen strain He/80),
170 recombinant BDV in which the two serine residues in position 26 and 28 of BDV-P were
171 replaced by alanine residues (rBDV- P_{AA}) or recombinant wild-type BDV (rBDV-Pwt),
172 composed of the canonical sequence of wild-type BDV strain He/80 (19). Cells were grown
173 in Dulbecco's modified Eagle's medium supplemented with 10 % fetal bovine serum and 2
174 mM L-glutamine. For HEK-293T cells, 2 mg/ml geneticin was added to the medium.

175 Lentiviral vector plasmids allowing expression of BDV N or wild type or mutant BDV
176 P under the control of the CAG promoter were engineered by insertion of viral gene
177 sequences into *Bam*HI/*Xho*I restriction sites of the pTrip-CAG plasmid (kind gift of Dr
178 Charneau). Non-replicative vector particles were produced by transient transfection of HEK-
179 293T cells with each vector plasmid, the second generation psPAX2 packaging plasmid
180 (Addgene plasmid 12260, provided by D. Trono) and pMD2.G plasmid encoding the
181 vesicular stomatitis virus envelope glycoprotein (VSV-G, Addgene plasmid 12259, provided
182 by D. Trono). Particles were concentrated from cell culture supernatants by
183 ultracentrifugation. Gene transfer titers were determined on transduced HEK-293T cells by
184 indirect immunofluorescence using anti-BDV N or P protein sera.

185 For the establishment of Vero cell lines stably expressing individual BDV proteins,
186 Vero cells were transduced by lentiviral vectors at a multiplicity of transduction of 10. A
187 lentiviral vector encoding green fluorescent protein (GFP) was used to establish the control
188 cell line. For each cell line, transduction efficacy was assessed by immunofluorescence, to
189 ensure that at least 95 % of the cells expressed the protein of interest.

190

191 **Histone preparation and western blot analysis.** The procedure for histone preparation was
192 adapted from Shechter et al. (20). Nuclei were isolated upon cell lysis in a hypotonic buffer
193 containing 0.2 % Triton-X100, 20 mM β -glycerophosphate, 10 mM Hepes pH 7.6, 1.5 mM
194 MgCl₂, 10 mM KCl, 10 mM sodium butyrate, 1 mM DTT and protease inhibitors (Complete
195 Mini, Roche). After centrifugation and washing, nuclei were incubated in 0.4 N HCl during
196 1 h at 4°C to allow histone solubilization. After removal of the nuclear debris by
197 centrifugation, histones were precipitated from supernatant by the addition of 4 volumes of
198 acetone and incubation overnight at -20°C. They were then centrifuged at 15,000 X g during
199 20 min and histone-enriched pellets were resuspended in Laemmli buffer for western blot
200 analysis. Western blots were performed as previously described (19) using either histone
201 preparations or whole cell extracts and the following primary antibodies: anti total H2B,
202 H2B acetyl K5, H2B acetyl K12, H2B acetyl K15, H2B acetyl K20, H3 pan acetyl, total H3
203 and H4 acetyl K8 from Epitomics (rabbit monoclonal antibodies); anti total H4, H4 tetra-
204 acetyl, H4 acetyl K5, H4 acetyl K12 and H4 acetyl K16 from Active Motif (rabbit
205 antibody); rabbit antisera anti BDV N and P proteins (21) and mouse monoclonal anti actin
206 (Sigma). The secondary antibodies used were anti-rabbit and anti-mouse antibodies coupled
207 to 680 nm and 770 nm infrared dyes (Biotium). Laser scanning of blots and quantitative
208 analyses were performed using the Odyssey Infrared Imaging System (Li-Cor).
209 Quantification of histone acetylation level was carried out by measuring the intensity of the
210 signal corresponding to the acetylated histone normalized by the corresponding signal for
211 total histone. Results were expressed as variation of acetylation compared to the mean level
212 of control cells (uninfected or mock transfected/transduced), which was set to 1. Data are
213 presented as means \pm SEM. Statistical significance was determined using paired t-test.

214

215 **Indirect immunofluorescence analysis.** Cells were fixed with 2 % paraformaldehyde at
216 room temperature for 10 min followed by 4 % paraformaldehyde for 10 min. They were
217 washed 3 times in PBS (Invitrogen), and permeabilized with PBS 0.1 % Triton-X100 during
218 4 min. Cells were washed twice in PBS, blocked in 2.5 % normal goat serum (Invitrogen)
219 during at least 1 h. Primary antibodies (the same used for western blot analyses described
220 above) were diluted in PBS containing 2.5 % normal goat serum and incubated 1 h at room
221 temperature. For controlling infection, transduction or transfection efficiencies, we used
222 rabbit antisera raised against BDV N or BDV P proteins (21). To assess neuronal integrity,
223 we used a mouse anti β III-Tubulin antibody (Sigma). Upon incubation with primary
224 antibodies, cells were washed 3 times with PBS 0.1 % Triton-X100 and incubated with

225 secondary goat anti rabbit antibody coupled to Alexa Fluor 488 or goat anti mouse antibody
226 coupled to Alexa Fluor 594, during 1 h at room temperature. After 3 washes, coverslips
227 were mounted onto microscope slides using ProLong Gold (Invitrogen) containing DAPI.
228 To measure histone acetylation levels, images were acquired on a LSM 510 confocal
229 microscope (Zeiss) using fixed acquisition parameters. The Imaris software (Bitplane AG,
230 Switzerland) was used to automatically calculate the mean density of fluorescence signals
231 for individual cells, after background subtraction and thresholding. The same parameters
232 were used for the quantification of each picture. To assess BDV N and P protein expression,
233 images were acquired on a Zeiss Apotome microscope.

234

235 **Analysis of HAT and HDAC activities.** Nuclear extracts were prepared using a
236 commercially available kit (Active Motif) and protein concentrations were determined by
237 Bradford assays. Equal amounts of each extracts were then used to measure HAT and
238 HDAC enzymatic activities, by using the HAT Assay Kit and the HDAC Assay Kit (Active
239 Motif). For each reaction, 2 µg of nuclear extracts were used for HAT assays and 4 µg of
240 nuclear extracts for HDAC assays. Reactions were systematically carried out in duplicate for
241 each extract. Revelation of the assay was done by fluorescence quantification using a
242 Varioskan Flash scanner (Thermo Scientific).

243

244 **Analysis of BDV multiplication and protein expression by flow cytometry.** 4.10^5 Vero
245 cells were plated and infected with cell-free BDV at a multiplicity of infection of 0.5. They
246 were treated with 1 mM sodium butyrate (Sigma) or 10 µM anacardic acid (Tocris
247 bioscience) the same day of infection and again 48 h later. After 4 days of incubation, cells
248 were dissociated with trypsin, harvested, and fixed in 2 % paraformaldehyde for 15 min at
249 room temperature. After fixation, cells were permeabilized during 20 min with FACS buffer
250 containing 0.5 % saponin, 1 % bovine serum albumin and 3 mM EDTA. Cells were then
251 incubated in blocking buffer (3 % pre-immune rabbit serum diluted in FACS buffer) during
252 1 h before addition of 5 µg/mL of antibodies for 1 h at 4 °C. Anti BDV P and isotype control
253 antibodies were purified from rabbit sera (Abselect Serum Antibody Purification System,
254 Innova Biosciences) and pre-conjugated with an Atto-488 fluorescent label (Lightning-Link
255 Conjugation System, Innova Biosciences). After extensive washes, flow cytometry data
256 were collected on a FACSCalibur (BD Biosciences) and analyzed using FlowJo software
257 (TreeStar, version 8.8.6).

258

259 **Reverse-transcription and quantitative PCR for measurement of vRNA.** 10^5 Vero cells
260 were plated and infected with cell-free BDV at a multiplicity of infection of 0.5. At different
261 times post infection, total RNA were prepared from cells using the Nucleospin kit
262 (Macherey-Nagel) following the manufacturer's instructions. One μg of RNA was reverse-
263 transcribed using SuperScript III Reverse Transcriptase (Life Technologies) with a primer
264 specific for genomic viral RNA (primer sequence: 5'GACACTACGACGGGAACGAT3').
265 The resulting cDNAs were used for quantitative PCR (qPCR) experiments with primers
266 specific for BDV genome (forward primer: 5'CGGTAGACCAGCTCCTGAAG3', reverse
267 primer: 5'GAGGTCCACCTTCTCCATCA3'). In parallel, one μg of RNA was reverse-
268 transcribed using random hexamers to amplify total cDNAs. These cDNAs were used for
269 qPCR using primers specific for glyceraldehyde 3 phosphate deshydrogenase (GAPDH) for
270 normalization (forward primer: 5'CAATGACCCCTTCATTGACC3', reverse primer:
271 5'GACAAGCTTCCCGTTCTCAG3'). qPCR reactions were prepared with LightCycler 480
272 DNA SYBR Green I Master reaction mix (Roche Diagnostics) and run in duplicate on a
273 LightCycler 480 instrument (Roche Diagnostics). Viral genome quantification was
274 expressed in arbitrary units according to the following formula: amount of vRNA = $2^{-(Ct_{BDV} -$
275 $Ct_{GAPDH})}$.

276

277 **Results**

278

279 **BDV infection decreases histone acetylation of specific lysine residues.** To assess the
280 impact of BDV infection on histone acetylation patterns, primary neuronal cultures were
281 infected or not by BDV. Neurons were cultured for 14 days, a time sufficient to allow BDV
282 spreading to all neurons, as verified by indirect immunofluorescence analysis (data not
283 shown) and in agreement with our previous proteomics findings (21, 22). There was no
284 overt impact of infection on the morphology or viability of the cultures, consistent with the
285 non-cytolytic replication strategy of BDV. From these neurons, we prepared histone
286 fractions (20), which were analyzed by western blot using antibodies targeting each known
287 acetylatable lysine of H2B (Figure 1A, left panel). We observed that BDV infection led to a
288 significant decrease of H2B acetylation on K5 and K20 (33 and 26 % decrease, respectively,
289 Figure 1A), consistent with our previous findings (9). In addition, infection also induced a
290 decrease of acetylation on K15, but not on K12. We next asked whether this acetylation
291 defect was restricted to H2B or could be extended to two other core histones, H3 and H4, for

292 which acetylation modifications have been extensively described (23). While global levels
293 of H3 acetylation were unchanged by infection, a significant decrease of the global
294 acetylation level of H4 was observed in infected neurons (Figure 1B), which was
295 attributable to decreased acetylation of K5, K8 and K16 but not of K12 (Figure 1C).

296 As BDV is able to infect a wide variety of cell types *in vitro*, even from non-neuronal
297 origin, we next asked whether this histone acetylation decrease was also observed in other
298 cell types. To this aim, histone acetylation levels were evaluated in Vero cells persistently
299 infected by BDV (Vero-BV (24)). We observed that histone acetylation levels were also
300 decreased in Vero-BV cells and that, remarkably, it occurred exactly on the same lysine
301 residues than in primary neuronal cultures (Figure 2). Interestingly, changes were even more
302 pronounced, reaching around 40 to 50 % decrease depending on the lysine, presumably
303 resulting from the fact that Vero-BV cells had been infected for numerous passages. As for
304 neurons, there was no change in acetylation of H2B K12 or H4 K12, neither in global H3
305 acetylation, suggesting that BDV may impact a general process conserved in several cell
306 types that selectively targets the acetylation status of specific lysine residues of H2B and H4.

307 To confirm our findings concerning the impact of BDV infection on histone acetylation
308 using a different approach, we performed indirect immunofluorescence analysis of histone
309 acetylation using Vero and Vero-BV cells. As shown in Figure 3, this analysis revealed a
310 general decrease of fluorescence levels in infected cells when we assessed H2B acetylation
311 on K5, K15 and K20, but not for K12, in perfect agreement with our western blot results.
312 This experiment also revealed that the decrease of acetylation was similar in all cells (Figure
313 3, right panels) and thus was a global effect resulting from BDV infection.

314

315 **BDV P is responsible for histone acetylation decrease.** We next assessed which of the
316 BDV-encoded proteins could be responsible for this acetylation decrease. Among these,
317 BDV N and BDV P represent potential candidates for decreasing histone acetylation. Indeed,
318 they belong to the RNP complex and are abundant in the nucleus of infected cells, where
319 they locate in close association with chromatin (1). To identify which of these two proteins
320 could account for decreased histone acetylation, plasmids encoding BDV N or BDV P were
321 transfected using the Amaxa technology that allows a high rate of transfection for primary
322 neuronal cultures without altering viability. Fourteen days after transfection, we verified that
323 neuronal integrity was indeed preserved using immunofluorescence analysis for β III-Tubulin.
324 Moreover, at least 75 % of neurons expressed the transfected BDV protein (Figure 4A). We
325 also observed that both BDV N and BDV P were expressed predominantly in the nucleus of

326 transfected neurons, consistent with the presence of nuclear localization signals in both
327 proteins (25, 26) (Figure 4A). Analysis of histone acetylation levels in transfected neurons
328 was compared to levels in neurons transfected with an empty plasmid. As shown in Figure
329 4B for the acetylation of H2B K20, we observed that the singled-out expression of BDV P
330 into primary neurons led to decreased histone acetylation levels, a result that was not
331 observed for BDV N-expressing neurons (Figures 4B and 4C). This experiment was
332 reproduced for each lysine residue analyzed previously and results are summarized in Table
333 1. Strikingly, the isolated expression of BDV P in neurons had the same impact on histone
334 acetylation than BDV infection, with the same lysine specificity and at the same level of
335 decrease. In order to verify if the same findings were observed in non-neuronal cells, we
336 generated stable Vero cell lines expressing each of the viral candidate proteins, or GFP as a
337 control, and analyzed histone acetylation (Table 2). Acetylation of the different lysine
338 residues of H2B and H4 was drastically and significantly reduced only in the cell line
339 expressing BDV P, confirming that BDV P is responsible for decreased histone acetylation
340 in a non-neuronal cell line. These data indicate that BDV P is the key viral determinant
341 responsible for the decrease of histone acetylation during BDV infection.

342

343 **BDV P binding to HMGB-1 is not required for decreased histone acetylation.** One
344 feature of BDV P is its ability to bind chromatin via its interaction with HMGB-1, a non-
345 histone architectural protein of the chromatin (1, 27). Given the important roles of HMGB-1
346 on chromatin dynamics (28), we next reasoned that the impact of BDV P on histone
347 acetylation might be dependent on its interaction with HMGB-1. To test this hypothesis, we
348 used a mutant form of BDV P, BDV P_{E84N}, which no longer binds to HMGB-1 due to a
349 mutation in its interaction domain (1). As described above, primary neuronal cultures were
350 transfected with plasmids encoding wild-type BDV P, the BDV P_{E84N} mutant, or an empty
351 plasmid, and we next analyzed histone acetylation levels (Figure 5). Indirect
352 immunofluorescence analysis indicated that the transfection efficiency was around 80 % and
353 that the mutant BDV P_{E84N} still localized into the nucleus (Figure 5A). When using H2B
354 K20 acetylation as a read-out, we observed that acetylation was still inhibited in neurons
355 expressing the BDV P_{E84N} mutant (Figure 5B). Thus, interaction of BDV P with chromatin
356 via its binding to HMGB-1 appears dispensable for the protein to exert its action on histone
357 acetylation.

358

359 **BDV P phosphorylation by PKC is essential for its action on histone acetylation.**
360 Similarly to other non-segmented negative-strand RNA viruses, BDV P is a subunit of the
361 viral polymerase complex and its activity is regulated upon phosphorylation by host kinases.
362 BDV P is preferentially phosphorylated at serine residues 26 and 28 by PKC and, to a lesser
363 extent, at serine residues 70 and 86 by casein kinase II (29, 30). PKC phosphorylation is of
364 particular interest for BDV pathogenesis, since we previously showed that BDV P acts as a
365 PKC decoy substrate and impairs synaptic plasticity by diverting PKC from its natural
366 targets in neurons (21, 22). Interestingly, PKC also regulates histone acetylation levels,
367 notably by controlling activity of cellular histone acetyl transferases (HATs) (31, 32). Thus,
368 we next asked whether BDV P phosphorylation by PKC was required for its impact on
369 histone acetylation.

370 To this aim, we used the PKC non-phosphorylatable BDV P_{AA} mutant, in which the two
371 serine residues at positions 26 and 28 of BDV P had been replaced by alanine (A) residues
372 (22). We used transfected primary neuronal cultures (Figure 6A), as well as Vero cell lines
373 stably expressing wild type or mutant BDV P (Figure 6B). In addition, we also used Vero
374 cells persistently infected by recombinant BDV (rBDV) expressing wild type or mutant P_{AA}
375 (Figure 6C) (22). In each case, BDV P_{AA} subcellular localization was assessed by indirect
376 immunofluorescence and was similar to that of the wild type protein (Figure 6, left panels).
377 Histone preparations from these different cells were analyzed for acetylation levels by
378 western blot (Figure 6, right panels for H2B K20 acetylation). In all experimental models,
379 the BDV P_{AA} mutant had lost the ability to inhibit histone acetylation. Moreover, results
380 were similar when measurement of acetylation was done with anti acetylated H2B K5 and
381 anti pan acetylated H4 antibodies (data not shown). Therefore, phosphorylation of BDV P
382 by PKC is mandatory to mediate decrease of histone acetylation.

383

384 **Impaired histone acetylation due to BDV infection results from inhibition of neuronal**
385 **HAT activities.** Histone acetylation is a dynamic, enzyme-regulated process, which results
386 from the balance between activities of HATs and histone deacetylases (HDACs), two wide
387 families of enzymes acting in concert (33, 34). To examine whether BDV infection perturbs
388 the equilibrium between these two families, enzymatic assays were performed to evaluate
389 cellular HAT and HDAC activities, using nuclear extracts prepared from non-infected or
390 infected primary neuronal cultures. Levels of HDAC activities were similar in nuclear
391 preparations from infected or non-infected neurons (Figure 7A). In contrast, HAT activities
392 were significantly decreased in nuclear extracts from BDV-infected neurons, reaching a

393 level of about 25 % of decrease (Figure 7B). The reduced histone acetylation levels
394 consecutive to BDV infection are thus due to inhibition of acetylation rather than increased
395 deacetylation. We next assessed whether the BDV P expressed alone in primary cortical
396 neurons could also inhibit the cellular HAT enzymatic activities. Nuclear extracts prepared
397 from mock or BDV P transfected neurons were used to perform HAT enzymatic assays as
398 described above (Figure 7C). Isolated expression of wild-type BDV P in neurons led to an
399 inhibition of HAT activities at similar level than infection (around 25%). This effect was
400 partly reverted, although not entirely, in neurons expressing the non-phosphorylable BDV
401 P_{AA} mutant (Figure 7C). Thus, the BDV P protein mediates inhibition of cellular HAT
402 enzymatic activities and its phosphorylation by PKC may be implicated in this inhibition.

403

404 **HAT and HDAC inhibitors modulate BDV replication.** Having shown that BDV
405 infection modifies the histone acetylation pattern by inhibiting cellular HAT activities, we
406 next investigated whether such modifications would help to create a more favorable milieu
407 for viral replication. To examine the interplay between cellular acetylation levels and BDV
408 replication, HAT and HDAC activities were pharmacologically modulated and the resulting
409 consequences on BDV replication were followed at different times post-infection. We used
410 sodium butyrate, an inhibitor of HDAC activities (35) and anacardic acid, an inhibitor of
411 HAT activities (36) to treat Vero cells that were concomitantly infected by BDV. We first
412 checked that the two drugs did not affect cell viability at the concentrations used during the
413 experiments (data not shown). We also verified that both inhibitors indeed modulated
414 histone acetylation levels in non-infected cells when compared to untreated cells (Figure
415 8A). Four days after onset of treatment, anacardic acid induced a 50 % decrease of H2B K20
416 acetylation compared to control cells (Figure 8A), a level similar to that observed during
417 BDV infection (Figure 2). In contrast, sodium butyrate treatment led to a large increase
418 (seven-fold) of H2B K20 acetylation.

419 To measure the impact of drug treatment on viral replication, Vero cells were
420 harvested four days after infection and percentages of infected cells were determined by
421 flow cytometry upon cell staining with an anti BDV P antibody. The data presented in
422 Figure 8B, representative for three independent experiments, indicate that without drug
423 treatment, 75 % of cells were positive for BDV P (Figure 8B, up panel). The percentage of
424 infected cells dropped at 62 % upon treatment with anacardic acid, indicating that viral
425 dissemination into the culture was reduced compared to control cells (Figure 8B, down
426 panel). Moreover, the mean fluorescence intensity value (MFI), reflecting the amount of

427 synthesized BDV P, was lower in anacardic acid-treated cells compared to untreated cells (8
428 vs. 14), suggesting that expression of viral proteins was also decreased following this
429 treatment. In contrast, sodium butyrate-treated cells displayed strong enhanced viral
430 dissemination, with 94 % of infected cells four days post-infection (Figure 8B, middle
431 panel), and a very efficient expression of BDV P in infected cells as indicated by the MFI
432 value of 41. In parallel, we also assessed expression of BDV N and P proteins in non-treated
433 or treated cells by western blot. A progressive reduction of BDV N and P protein expression
434 was observed in anacardic acid-treated cells, in agreement with flow cytometry data. In
435 contrast, BDV protein expression was enhanced in sodium butyrate-treated cells. Finally, we
436 also conducted qRT-PCR assays to measure viral RNA (vRNA) production. vRNA levels
437 were measured each day post-infection during four days, in non-treated, sodium butyrate- or
438 anacardic acid-treated Vero cells (Figure 8D). Inhibition of cellular HATs by anacardic acid
439 led to a 50 % reduction of BDV vRNA four days post infection, whereas HDAC inhibition
440 by sodium butyrate allowed a 2.5 fold enhancement of vRNA amounts at the same time
441 point. Altogether, these results indicate that replication of BDV is positively correlated with
442 histone acetylation levels, a lower level of viral replication being observed when histone
443 acetylation levels are reduced.

444

445 **Discussion**

446

447 The objective of this study was to gain insight on the outcome of the intra-nuclear
448 persistence of a RNA virus, such as BDV, on the host cell chromatin dynamics. Here, we
449 demonstrate that BDV infection leads to a significant decrease of histone acetylation on
450 selected lysine residues. We also show that this decrease is due to inhibition of cellular HAT
451 activities, mediated by the viral phosphoprotein, and that P phosphorylation by PKC plays a
452 role in its effect. Finally we show that manipulation of host cell epigenetics leads to
453 modulation of viral replication (Figure 9). These data illustrate a novel and fascinating
454 example of virus/host cell interaction, which could be a strategy to favor long lasting BDV
455 persistence. This strategy, different from classical latency, would rely on "self-restriction" of
456 replication. This would prevent exhaustion of the host cell consecutive to an excessive
457 recruitment of host factors, thus limiting cellular damage.

458 This acetylation decrease, which could seem moderate at first, was however consistently
459 observed both in primary neurons and established cell lines. The observed levels of

460 reduction (around 30 %) are actually close to levels observed in neurons from mice knock-
461 out for the CREB Binding Protein (CBP) HAT, which display clear memory defects (37, 38).
462 Interestingly, our observation that the exact same lysine residues were affected in all cell
463 types argues for a conserved mechanism of inhibition in neuronal and non-neuronal cells.
464 Interestingly, decreases of histone acetylation were more important in persistently infected
465 Vero cells than in neurons, infected for 14 days, suggesting that BDV persistence into the
466 host cell may potentiate the inhibition of histone acetylation. A recent SILAC-based analysis
467 of the impact of BDV infection on the proteome of human oligodendroglial cells also
468 revealed changes in histone lysine acetylation patterns (39). This study reported similar
469 decreased values for certain lysine residues, but also many differences, in particular for H2B
470 K15 for which an increase of acetylation was observed. It would be interesting to determine
471 whether such differences are due to divergences in cell types or viral strains.

472 In our study, the decrease of histone acetylation due to BDV infection appeared to be
473 restricted to specific H2B and H4 lysine residues. It would be interesting in the future to
474 determine their genome-wide distribution, similar to what has been reported for adenovirus
475 E1a protein (40). In this case, ChIP-sequencing experiments revealed that the global
476 decrease of acetylation on H3 K18 observed during infection was correlated to a
477 redistribution of acetylation at the genome scale, with enrichment in promoter regions of
478 genes needed for cell replication.

479 Our results unambiguously demonstrated that BDV P, by inhibiting cellular HAT
480 activities, was responsible for decreased histone acetylation, even when expressed alone,
481 thereby pointing to a new role for this multifunctional protein that lies at the crossroads
482 between BDV and numerous cellular pathways (22, 41, 42). Interestingly, the impact of
483 BDV P on histone acetylation appears to be dissociated from its interaction with chromatin,
484 in particular from its binding to HMGB-1, as revealed by the use of the BDV P_{E84N} mutant,
485 although we did not formally test that this was true for all lysine residues affected by BDV
486 and only used H2B K20 as a read-out. This fact is consistent with our recent results using
487 real-time live cell imaging, which showed that BDV P is actually highly mobile in vSPOTs,
488 suggesting a labile and transitory interaction with chromatin that may not be sufficient to
489 directly interfere with chromatin dynamics (8).

490 In contrast, invalidation of the PKC phosphorylation sites on BDV P completely
491 abrogated its impact on histone acetylation and, at least partially, on HAT activities. This
492 may be due to a direct interference of phosphorylated P on HAT activities. Alternatively,
493 BDV P could serve as a PKC decoy substrate, in agreement with our previous findings (21,

494 22) and divert PKC from one or several HATs. Indeed it is known that the enzymatic
495 activities of several HATs can be positively or negatively regulated by PKC (31, 43-46).
496 Such a mechanism would differ from what has been described for other viruses such as
497 adenovirus, for which the viral protein E1a directly binds the CBP/p300 HAT (10). Another
498 example is influenza virus, for which it was shown that the non-structural protein-1
499 possesses a histone-like sequence that serves as mimic substrate for the Tip60 HAT (47).
500 Since restoration of HAT activities were not complete with the P_{AA} mutant, we thus cannot
501 formally exclude the possibility that other functions controlled by P may also play a role.

502 The characterization of which HAT(s) are actually impacted by BDV P will be
503 challenging. Only little is known concerning the post-translational modifications of most
504 HATs, which are often very large proteins with many potentially modifiable residues (48).
505 Moreover, although PKC can phosphorylate several HATs (44, 45), the resulting impact on
506 their activities, combined with other post-translational modifications, is poorly understood.
507 The fact that the pattern of impaired histone lysine acetylation was remarkably similar
508 amongst cell types could provide some clues for a future identification of the HATs,
509 although most of them present a broad specificity for their substrates and could thus
510 virtually acetylate the vast majority of histone lysine residues (23).

511 The role of BDV P phosphorylation in viral replication is still incompletely understood.
512 Phosphorylation mutants of BDV P display increased polymerase activity in minireplicon
513 assays, whereas they induce cell-type dependent impaired viral spread, leading to the
514 hypothesis that P might play multiple and contrasted roles in the viral cycle (19, 29).
515 Similarly, it has been shown that phosphorylation of Ebolavirus VP30 protein plays opposite
516 roles in viral replication and transcription (49). Here, we demonstrate that the P_{AA} mutant
517 protein has lost the capacity to reduce histone acetylation, whereas it has been shown to
518 increase viral RNA polymerase activity (19, 29). These results are thus in agreement with
519 our findings that BDV replication is favored when level of cellular histone acetylation is
520 higher.

521 Finally, epigenetic modifications, in particular histone acetylation, have now emerged
522 as central regulators of cognitive processes during learning and memory (16, 50). Hence,
523 impaired histone acetylation occurring in the brain of BDV-infected animals may participate
524 to behavioral perturbations observed in BDV-infected hosts (4). We are currently assessing
525 the impact on cognition of the isolated expression of BDV P in neurons in order to expand
526 results obtained in transgenic mice expressing BDV P in astrocytes (51). These data may
527 reveal for the first time that an animal virus, or a singled-out viral protein, can perturb

528 cognitive functions by interfering with PKC-dependent and neuronal epigenetic signaling
529 pathways.

530

531 **Acknowledgments**

532

533 We thank the staff of the different facilities of our research center (imaging and flow
534 cytometry platforms) for excellent assistance that was instrumental for the proper realization
535 of this project. We thank D. Trono and P. Charneau for lentiviral vector plasmids. We are
536 grateful to Stéphane Chavanas, Roland Liblau and Abdelhadi Saoudi for critical reading of
537 the manuscript and insightful comments.

538

539 **Funding**

540

541 This work was supported by grants from ANR (ANR-10-Blanc-1322, to DGD), the
542 Fondation pour la Recherche Médicale (Equipe FRM 2009, to DGD), a grant from the
543 Toulouse III University research council (to CEM) and institutional grants from Inserm and
544 CNRS (to DGD). This work is part of the Ph.D. thesis work of EMB, who was supported by
545 a doctoral fellowship from the Ministère de l'Enseignement Supérieur et de la Recherche.

546

547 **Author Contributions**

548

549 Conceived and designed the experiments: EMB, MS, DGD, CEM. Performed the
550 experiments: EMB, MS, AB, AT, CF, CEM. Analyzed the data: EMB, MS, CEM. Wrote the
551 paper: DGD, CEM.

552

553 **References**

554

- 555 1. **Matsumoto Y, Hayashi Y, Omori H, Honda T, Daito T, Horie M, Ikuta K,**
556 **Fujino K, Nakamura S, Schneider U, Chase G, Yoshimori T, Schwemmle M,**
557 **Tomonaga K.** 2012. Bornavirus closely associates and segregates with host
558 chromosomes to ensure persistent intranuclear infection. *Cell Host & Microbe*
559 **11:492-503.**
- 560 2. **Lipkin WI, Briese T, Hornig M.** 2011. Borna disease virus - fact and fantasy. *Virus*
561 *Res.* **162:162-172.**

- 562 3. **Gonzalez-Dunia D, Volmer R, Mayer D, Schwemmle M.** 2005. Borna disease
563 virus interference with neuronal plasticity. *Virus Res.* **111**:224-234.
- 564 4. **Pletnikov MV, Moran TH, Carbone KM.** 2002. Borna disease virus infection of
565 the neonatal rat: developmental brain injury model of autism spectrum disorders.
566 *Front Biosci* **7**:D593-607.
- 567 5. **Carbone KM, Rubin SA, Nishino Y, Pletnikov MV.** 2001. Borna disease: virus-
568 induced neurobehavioral disease pathogenesis. *Curr Opin Microbiol* **4**:467-475.
- 569 6. **Horie M, Honda T, Suzuki Y, Kobayashi Y, Daito T, Oshida T, Ikuta K, Jern P,**
570 **Gojobori T, Coffin JM, Tomonaga K.** 2010. Endogenous non-retroviral RNA virus
571 elements in mammalian genomes. *Nature* **463**:84-87.
- 572 7. **de la Torre JC.** 2002. Molecular biology of Borna disease virus and persistence.
573 *Front Biosci* **7**:d569-579.
- 574 8. **Charlier CM, Wu YJ, Allart S, Malnou CE, Schwemmle M, Gonzalez-Dunia D.**
575 2013. Analysis of borna disease virus trafficking in live infected cells by using a
576 virus encoding a tetracysteine-tagged p protein. *J Virol* **87**:12339-12348.
- 577 9. **Suberbielle E, Stella A, Pont F, Monnet C, Mouton E, Lamouroux L, Monsarrat**
578 **B, Gonzalez-Dunia D.** 2008. Proteomic analysis reveals selective impediment of
579 neuronal remodeling upon Borna disease virus infection. *J Virol* **82**:12265-12279.
- 580 10. **Horwitz GA, Zhang K, McBrien MA, Grunstein M, Kurdistani SK, Berk AJ.**
581 2008. Adenovirus small e1a alters global patterns of histone modification. *Science*
582 **321**:1084-1085.
- 583 11. **Paschos K, Allday MJ.** 2010. Epigenetic reprogramming of host genes in viral and
584 microbial pathogenesis. *Trends Microbiol.* **18**:439-447.
- 585 12. **Knipe DM, Lieberman PM, Jung JU, McBride AA, Morris KV, Ott M,**
586 **Margolis D, Nieto A, Nevels M, Parks RJ, Kristie TM.** 2013. Snapshots:
587 chromatin control of viral infection. *Virology* **435**:141-156.
- 588 13. **Gomez-Diaz E, Jorda M, Peinado MA, Rivero A.** 2012. Epigenetics of host-
589 pathogen interactions: the road ahead and the road behind. *PLoS Pathog* **8**:e1003007.
- 590 14. **Kim KY, Huerta SB, Izumiya C, Wang DH, Martinez A, Shevchenko B, Kung**
591 **HJ, Campbell M, Izumiya Y.** 2013. Kaposi's sarcoma-associated herpesvirus
592 (KSHV) latency-associated nuclear antigen regulates the KSHV epigenome by
593 association with the histone demethylase KDM3A. *J Virol* **87**:6782-6793.
- 594 15. **Hu J, Yang Y, Turner PC, Jain V, McIntyre LM, Renne R.** 2014. LANA binds to
595 multiple active viral and cellular promoters and associates with the
596 H3K4methyltransferase hSET1 complex. *PLoS Pathog* **10**:e1004240.
- 597 16. **Peixoto L, Abel T.** 2013. The role of histone acetylation in memory formation and
598 cognitive impairments. *Neuropsychopharmacology* **38**:62-76.
- 599 17. **Tsankova N, Renthal W, Kumar A, Nestler EJ.** 2007. Epigenetic regulation in
600 psychiatric disorders. *Nat Rev Neurosci* **8**:355-367.
- 601 18. **Chevalier G, Suberbielle E, Monnet C, Duplan V, Martin-Blondel G, Farrugia**
602 **F, Le Masson G, Liblau R, Gonzalez-Dunia D.** 2011. Neurons are MHC class I-
603 dependent targets for CD8 T cells upon neurotropic viral infection. *Plos Pathog*
604 **7**:e1002393.
- 605 19. **Schmid S, Metz P, Prat CM, Gonzalez-Dunia D, Schwemmle M.** 2010. Protein
606 kinase C-dependent phosphorylation of Borna disease virus P protein is required for
607 efficient viral spread. *Arch Virol* **155**:789-793.
- 608 20. **Shechter D, Dormann HL, Allis CD, Hake SB.** 2007. Extraction, purification and
609 analysis of histones. *Nature protocols* **2**:1445-1457.

- 610 21. **Volmer R, Monnet C, Gonzalez-Dunia D.** 2006. Borna disease virus blocks
611 potentiation of synaptic activity through inhibition of protein kinase C signaling.
612 *Plos Pathog* **2(3):e19**.
- 613 22. **Prat CM, Schmid S, Farrugia F, Cenac N, Le Masson G, Schwemmle M,**
614 **Gonzalez-Dunia D.** 2009. Mutation of the protein kinase C site in Borna disease
615 virus phosphoprotein abrogates viral interference with neuronal signaling and
616 restores normal synaptic activity. *PLoS Pathog* **5:e1000425**.
- 617 23. **Kouzarides T.** 2007. Chromatin modifications and their function. *Cell* **128:693-705**.
- 618 24. **Volmer R, Bajramovic JJ, Schneider U, Ufano S, Pochet S, Gonzalez-Dunia D.**
619 2005. Mechanism of the antiviral action of 1-beta-D-arabinofuranosylcytosine on
620 Borna disease virus. *J Virol* **79:4514-4518**.
- 621 25. **Shoya Y, Kobayashi T, Koda T, Ikuta K, Kakinuma M, Kishi M.** 1998. Two
622 proline-rich nuclear localization signals in the amino- and carboxyl-terminal regions
623 of the Borna disease virus phosphoprotein. *J. Virol.* **72:9755-9762**.
- 624 26. **Kobayashi T, Shoya Y, Koda T, Takashima I, Lai PK, Ikuta K, Kakinuma M,**
625 **Kishi M.** 1998. Nuclear targeting activity associated with the amino terminal region
626 of the Borna disease virus nucleoprotein. *Virology* **243:188-197**.
- 627 27. **Kamitani W, Shoya Y, Kobayashi T, Watanabe M, Lee BJ, Zhang G,**
628 **Tomonaga K, Ikuta K.** 2001. Borna disease virus phosphoprotein binds a neurite
629 outgrowth factor, amphoterin/HMG-1. *J Virol* **75:8742-8751**.
- 630 28. **Bustin M, Reeves R.** 1996. High-mobility-group chromosomal proteins:
631 architectural components that facilitate chromatin function. *Prog. Nucleic Acid Res.*
632 *Mol. Biol.* **54:35-100**.
- 633 29. **Schmid S, Mayer D, Schneider U, Schwemmle M.** 2007. Functional
634 characterization of the major and minor phosphorylation sites of the P protein of
635 Borna disease virus. *J Virol* **81:5497-5507**.
- 636 30. **Schwemmle M, De B, Shi LC, Banerjee A, Lipkin WI.** 1997. Borna disease virus
637 P-protein is phosphorylated by protein kinase c-epsilon and casein kinase II. *J. Biol.*
638 *Chem.* **272:21818-21823**.
- 639 31. **Wang J, Weaver IC, Gauthier-Fisher A, Wang H, He L, Yeomans J,**
640 **Wondisford F, Kaplan DR, Miller FD.** 2010. CBP histone acetyltransferase
641 activity regulates embryonic neural differentiation in the normal and Rubinstein-
642 Taybi syndrome brain. *Developmental cell* **18:114-125**.
- 643 32. **Clarke DL, Sutcliffe A, Deacon K, Bradbury D, Corbett L, Knox AJ.** 2008.
644 PKCbetaII augments NF-kappaB-dependent transcription at the CCL11 promoter via
645 p300/CBP-associated factor recruitment and histone H4 acetylation. *J. Immunol.*
646 **181:3503-3514**.
- 647 33. **Struhl K.** 1998. Histone acetylation and transcriptional regulatory mechanisms.
648 *Genes Dev.* **12:599-606**.
- 649 34. **Grunstein M.** 1997. Histone acetylation in chromatin structure and transcription.
650 *Nature* **389:349-352**.
- 651 35. **Candido EP, Reeves R, Davie JR.** 1978. Sodium butyrate inhibits histone
652 deacetylation in cultured cells. *Cell* **14:105-113**.
- 653 36. **Balasubramanyam K, Swaminathan V, Ranganathan A, Kundu TK.** 2003.
654 Small molecule modulators of histone acetyltransferase p300. *J Biol Chem*
655 **278:19134-19140**.
- 656 37. **Barrett RM, Malvaez M, Kramar E, Matheos DP, Arrizon A, Cabrera SM,**
657 **Lynch G, Greene RW, Wood MA.** 2011. Hippocampal focal knockout of CBP
658 affects specific histone modifications, long-term potentiation, and long-term memory.
659 *Neuropsychopharmacology* **36:1545-1556**.

- 660 38. **Chen G, Zou X, Watanabe H, van Deursen JM, Shen J.** 2010. CREB binding
661 protein is required for both short-term and long-term memory formation. *J Neurosci*
662 **30**:13066-13077.
- 663 39. **Liu X, Zhao L, Yang Y, Bode L, Huang H, Liu C, Huang R, Zhang L, Wang X,**
664 **Zhang L, Liu S, Zhou J, Li X, He T, Cheng Z, Xie P.** 2014. Human borna disease
665 virus infection impacts host proteome and histone lysine acetylation in human
666 oligodendroglia cells. *Virology* **464-465**:196-205.
- 667 40. **Ferrari R, Su T, Li B, Bonora G, Oberai A, Chan Y, Sasidharan R, Berk AJ,**
668 **Pellegrini M, Kurdistani SK.** 2012. Reorganization of the host epigenome by a
669 viral oncogene. *Genome Res.* **22**:1212-1221.
- 670 41. **Planz O, Pleschka S, Wolff T.** 2009. Borna disease virus: a unique pathogen and its
671 interaction with intracellular signalling pathways. *Cellular microbiology* **11**:872-879.
- 672 42. **Peng G, Yan Y, Zhu C, Wang S, Yan X, Lu L, Li W, Hu J, Wei W, Mu Y, Chen**
673 **Y, Feng Y, Gong R, Wu K, Zhang F, Zhang X, Zhu Y, Wu J.** 2008. Borna
674 disease virus p protein affects neural transmission through interactions with gamma-
675 aminobutyric acid receptor-associated protein. *J Virol* **82**:12487-12497.
- 676 43. **He L, Sabet A, Djedjos S, Miller R, Sun X, Hussain MA, Radovick S,**
677 **Wondisford FE.** 2009. Metformin and insulin suppress hepatic gluconeogenesis
678 through phosphorylation of CREB binding protein. *Cell* **137**:635-646.
- 679 44. **Wang J, Gallagher D, DeVito LM, Cancino GI, Tsui D, He L, Keller GM,**
680 **Frankland PW, Kaplan DR, Miller FD.** 2012. Metformin activates an atypical
681 PKC-CBP pathway to promote neurogenesis and enhance spatial memory formation.
682 *Cell stem cell* **11**:23-35.
- 683 45. **Yuan LW, Soh JW, Weinstein IB.** 2002. Inhibition of histone acetyltransferase
684 function of p300 by PKCdelta. *Biochim. Biophys. Acta* **1592**:205-211.
- 685 46. **Jin H, Kanthasamy A, Ghosh A, Yang Y, Anantharam V, Kanthasamy AG.**
686 2011. alpha-Synuclein negatively regulates protein kinase Cdelta expression to
687 suppress apoptosis in dopaminergic neurons by reducing p300 histone
688 acetyltransferase activity. *J Neurosci* **31**:2035-2051.
- 689 47. **Marazzi I, Ho JS, Kim J, Manicassamy B, Dewell S, Albrecht RA, Seibert CW,**
690 **Schaefer U, Jeffrey KL, Prinjha RK, Lee K, Garcia-Sastre A, Roeder RG,**
691 **Tarakhovsky A.** 2012. Suppression of the antiviral response by an influenza histone
692 mimic. *Nature* **483**:428-433.
- 693 48. **Legube G, Trouche D.** 2003. Regulating histone acetyltransferases and deacetylases.
694 *EMBO reports* **4**:944-947.
- 695 49. **Biedenkopf N, Hartlieb B, Hoenen T, Becker S.** 2013. Phosphorylation of Ebola
696 virus VP30 influences the composition of the viral nucleocapsid complex: impact on
697 viral transcription and replication. *J Biol Chem* **288**:11165-11174.
- 698 50. **Borrelli E, Nestler EJ, Allis CD, Sassone-Corsi P.** 2008. Decoding the epigenetic
699 language of neuronal plasticity. *Neuron* **60**:961-974.
- 700 51. **Kamitani W, Ono E, Yoshino S, Kobayashi T, Taharaguchi S, Lee BJ,**
701 **Yamashita M, Okamoto M, Taniyama H, Tomonaga K, Ikuta K.** 2003. Glial
702 expression of Borna disease virus phosphoprotein induces behavioral and
703 neurological abnormalities in transgenic mice. *Proc Natl Acad Sci U S A* **100**:8969-
704 8974.
- 705
706

707

708 **Figure legends**

709

710 **Figure 1. BDV infection decreases histone acetylation levels in primary neuronal**
711 **cultures.** A) Western blot analysis of H2B acetylation levels. Left panel: histone fractions
712 were prepared from parallel non-infected (NI) or infected (BDV) neuronal cultures and
713 analyzed by western blot with the indicated antibodies. Total H2B levels were assessed for
714 each sample and used to normalize acetylation signals. Right panel: Quantification of H2B
715 acetylation. Acetylation values (normalized for total H2B) obtained for infected neurons
716 were normalized to values obtained for non-infected neurons, which was set to 1 and which
717 is represented by the dashed line on the graph. Data are expressed as means \pm SEM from at
718 least nine independent sets of neuronal cultures. *, $P \leq 0.05$; **, $P \leq 0.01$; ***, $P \leq 0.001$; ns
719 = non significant, by paired t test. B) Analysis of global H3 and H4 acetylation by western
720 blot, done as in A). C) Analysis of acetylation on each H4 lysine residues by western blot,
721 done as in A).

722

723 **Figure 2. BDV infection decreases histone acetylation levels in persistently infected**
724 **Vero cells.** A) Analysis of H2B acetylation. Left panel: histone fractions were prepared
725 from parallel non-infected (NI) or persistently infected (BDV) Vero cells and analyzed by
726 western blot with the indicated antibodies. Total H2B levels were assessed for each sample
727 and used to normalize acetylation signals. Right panel: Quantification of H2B acetylation.
728 Acetylation values (normalized for total H2B) obtained for infected cells were normalized to
729 values obtained for non-infected cells, which was set to 1 and which is represented by the
730 dashed line on the graph. Data are expressed as means \pm SEM from at least seven
731 independent experiments, *i.e.*, cultures of Vero cells that were independently grown after the
732 original split during 5 to 20 passages. *, $P \leq 0.05$; **, $P \leq 0.01$; ***, $P \leq 0.001$; ns = non
733 significant, by paired t test. B) Analysis of H3 and H4 global acetylation by western blot,
734 done as in A). C) Western blot analysis of acetylation on each H4 lysine residues, done as in
735 A).

736

737 **Figure 3. Histone acetylation decrease due to BDV affects all infected cells.**
738 Immunofluorescence analysis was performed on non-infected (NI, left column) or
739 persistently infected (BDV, right column) Vero cells, in order to visualize acetylation on

740 H2B lysine residues, as indicated on the left of the figure. Bar = 25 μm . Fluorescence
741 quantification is presented on the right of each corresponding image. The mean signal
742 density per nucleus is expressed in arbitrary units (A. U.) and each spot corresponds to one
743 nucleus. Analyses are the sum of three cultures of Vero cells that were independently grown
744 after the original split during 5 to 20 passages, with more than 100 cells being analyzed for
745 each condition. ***, $P \leq 0.0001$, ns = non significant, by Mann-Whitney test.

746

747 **Figure 4. The BDV P protein is responsible for decreased histone acetylation levels.** A)
748 Indirect immunofluorescence analysis of primary neurons 14 days post-transfection.
749 Neurons were stained for DAPI, the viral BDV P or N proteins (green) and the neuronal
750 marker β III-tubulin (red). Merged images are shown on the right panels. Bar = 50 μm . B)
751 Western blot analysis, performed on nuclear extracts to visualize expression levels of BDV
752 P or N proteins (top panel; Empty = neurons transfected with an empty vector), and on
753 histone extracts to assess the level of K20 acetylated and total H2B (lower panels). C)
754 Quantification of H2B K20 acetylation levels in transfected neurons. Acetylation levels
755 (relative to total H2B) were normalized to values obtained for neurons transfected by an
756 empty plasmid, which was set to 1. Data are expressed as means \pm SEM obtained from at
757 least five independent sets of transfected neuronal cultures. **, $P \leq 0.01$, by paired t test.

758

759 **Figure 5. BDV P binding to HMGB-1 is dispensable for its impact on histone**
760 **acetylation.** A) Indirect immunofluorescence analysis of primary neurons 14 days post-
761 transfection. Neurons were stained for DAPI, the wild-type BDV P or P_{E84N} mutant protein
762 (green) and the neuronal marker β III-tubulin (red). Merged images are shown on the right
763 panel. Bar = 50 μm . B) Quantification of H2B K20 acetylation levels. Acetylation levels
764 (relative to total H2B) were normalized to values obtained for neurons transfected by an
765 empty plasmid, which was set to 1. Data are expressed as means \pm SEM from six
766 independent sets of transfected neuronal cultures. *, $P \leq 0.05$; **, $P \leq 0.01$, by paired t test.

767

768 **Figure 6. Mutation of the PKC phosphorylation sites of BDV P abrogates its action on**
769 **histone acetylation.** This analysis was performed in: A) transfected primary neuronal
770 cultures (control: empty vector), B) Vero cells stably expressing isolated proteins (control:
771 cell line expressing GFP) and C) Vero cells persistently infected by a recombinant BDV
772 (rBDV) wild type or encoding the mutant P_{AA} protein (control: non infected cells). Left

773 panels: indirect immunofluorescence analysis of BDV P_{wt} or P_{AA} expression in the different
774 cells. Cells were stained for DAPI and for wild-type BDV P or P_{AA} mutant protein (green).
775 Merged images are shown on the right. Bar = 50 μm. Right panels: comparative analysis of
776 H2B K20 acetylation levels in cells expressing wild-type BDV P or the BDV P_{AA} mutant. In
777 all cases, acetylation levels were normalized to levels obtained for control conditions, which
778 were set to 1 and which are indicated by a dashed line on the graphs. Data are expressed as
779 means ± SEM from at least four independent experiments (*i.e.*, independent sets of cultures
780 of transfected neurons or cultures of Vero cells that were independently grown after the
781 original split during 5 to 20 passages). **, $P \leq 0.01$ by paired *t* test.

782

783 **Figure 7. BDV infection and BDV P inhibit neuronal HAT activities.** Enzymatic assays
784 for dosing HDAC (A) and HAT (B and C) activities were performed using nuclear extracts
785 prepared from: non-infected (NI) or infected (BDV) primary neuronal cultures (A and B);
786 neurons transfected with an empty plasmid or plasmids encoding wild type BDV P or BDV
787 P_{AA} mutant (C). Enzymatic activities measured as described in the methods are expressed as
788 arbitrary units (A. U.). Data are the means ± SEM from at least four independent sets of
789 neuronal cultures. **, $P \leq 0.01$; *, $P \leq 0.05$, ns = non significant, by paired *t* test.

790

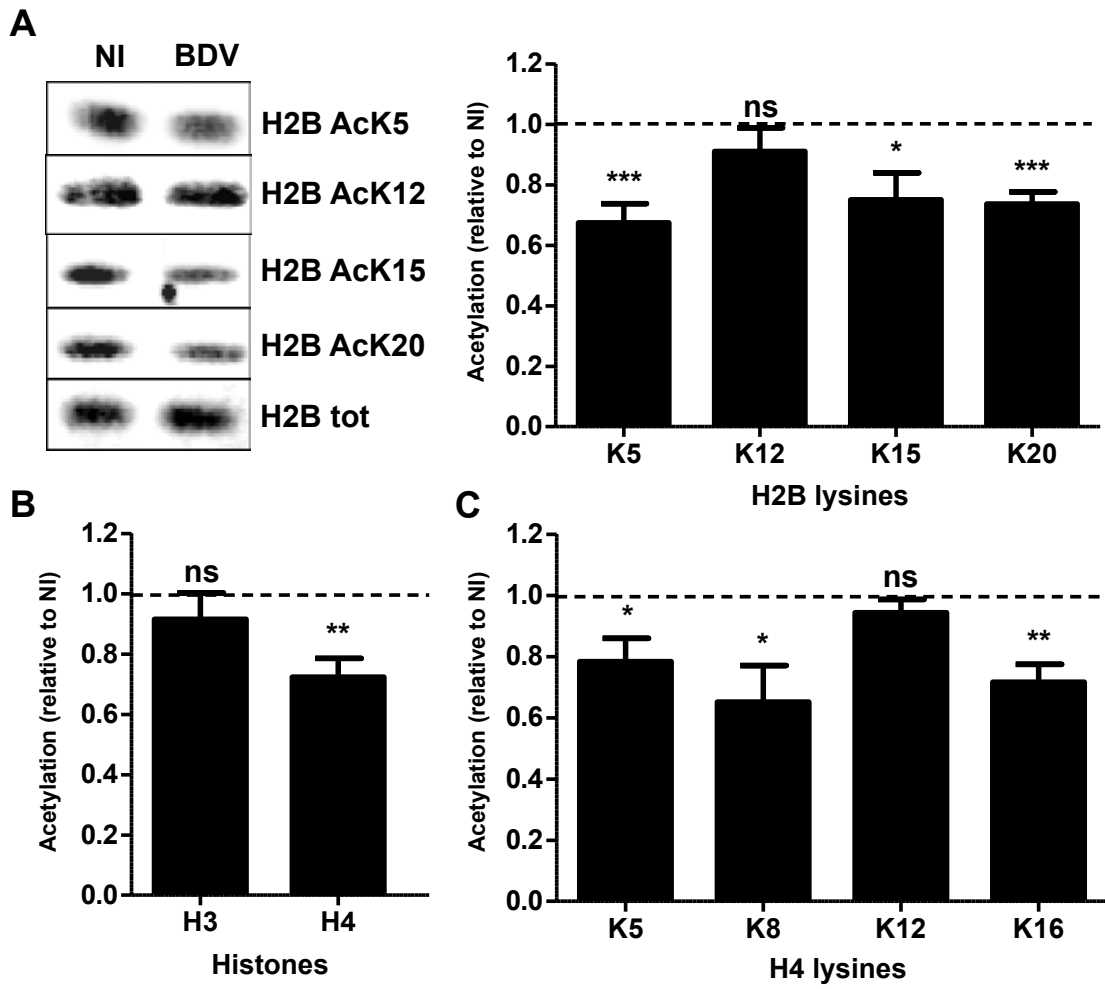
791 **Figure 8: HAT and HDAC inhibitors interfere with BDV replication.** Vero cells were
792 infected by BDV at a multiplicity of infection of 0.5, treated with 1 mM sodium butyrate
793 (NaBu) or 10 μM anacardic acid and followed daily for four days. Six independent sets of
794 de novo infection of Vero cells with cell-free BDV were performed. Out of these, three were
795 used for flow cytometry analysis and three to prepare protein/RNA extracts for western blots
796 and RT-qPCR. A) Impact of a 4-day treatment on H2B K20 acetylation levels using non-
797 infected cells. Acetylation levels (relative to total H2B) measured in treated cells were
798 normalized to values obtained for non-treated cells, which was set to 1. B) Flow cytometry-
799 based analysis of BDV spread in cell culture. Cells were stained with either control rabbit
800 IgG (black line) or rabbit anti-BDV P polyclonal IgG antibodies (grey full histogram).
801 Percentages of BDV P-positive cells and mean fluorescence intensities of this population
802 (MFI) are reported on the top and in the right bottom corner of the graphs, respectively. One
803 representative experiment out of three giving similar results is shown. C) Time-course
804 western-blot analysis (from day 1 (d1) to day 4 (d4)) of viral protein levels in cells that were
805 either left non-treated (NT), or treated with NaBu or anacardic acid (AA). The different

806 antibodies used are indicated on the right side of the western blots. Blots are from one
807 representative experiment out of three that gave similar results. D) Time-course (d1 to d4)
808 RT-qPCR analysis of vRNA levels using cells that were either left non-treated (NT), or
809 treated with NaBu or anacardic acid. Data are expressed as means \pm SEM from three
810 independent experiments. $P \leq 0.01$, by two-way ANOVA.

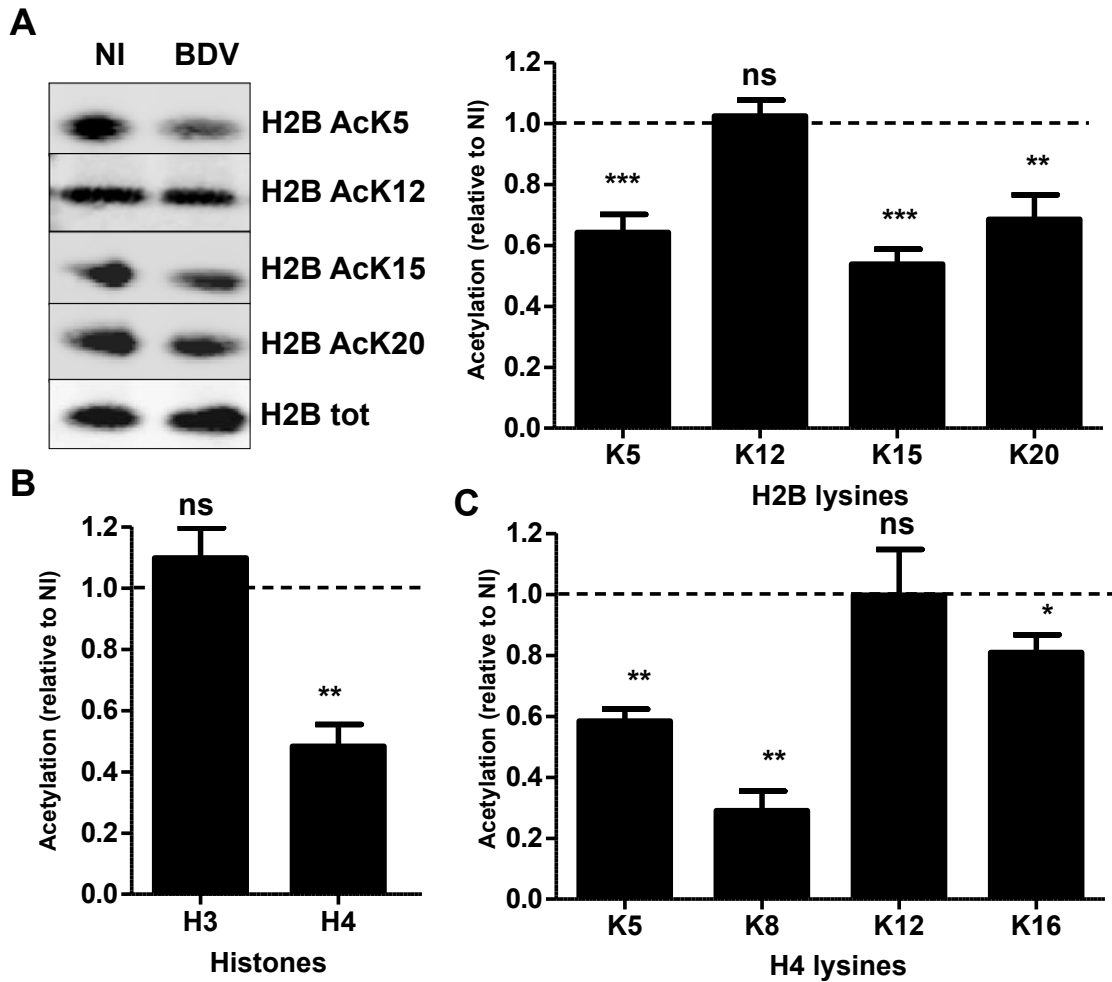
811

812 **Figure 9: A hypothetical model of BDV P-mediated manipulation of epigenetic**
813 **signaling.** During infection, BDV P decreases cellular HAT activities, partly upon its
814 phosphorylation by PKC, thereby resulting in lowered histone acetylation levels. Such
815 reduced histone acetylation levels would, in turn, lead to a reduced viral replication.

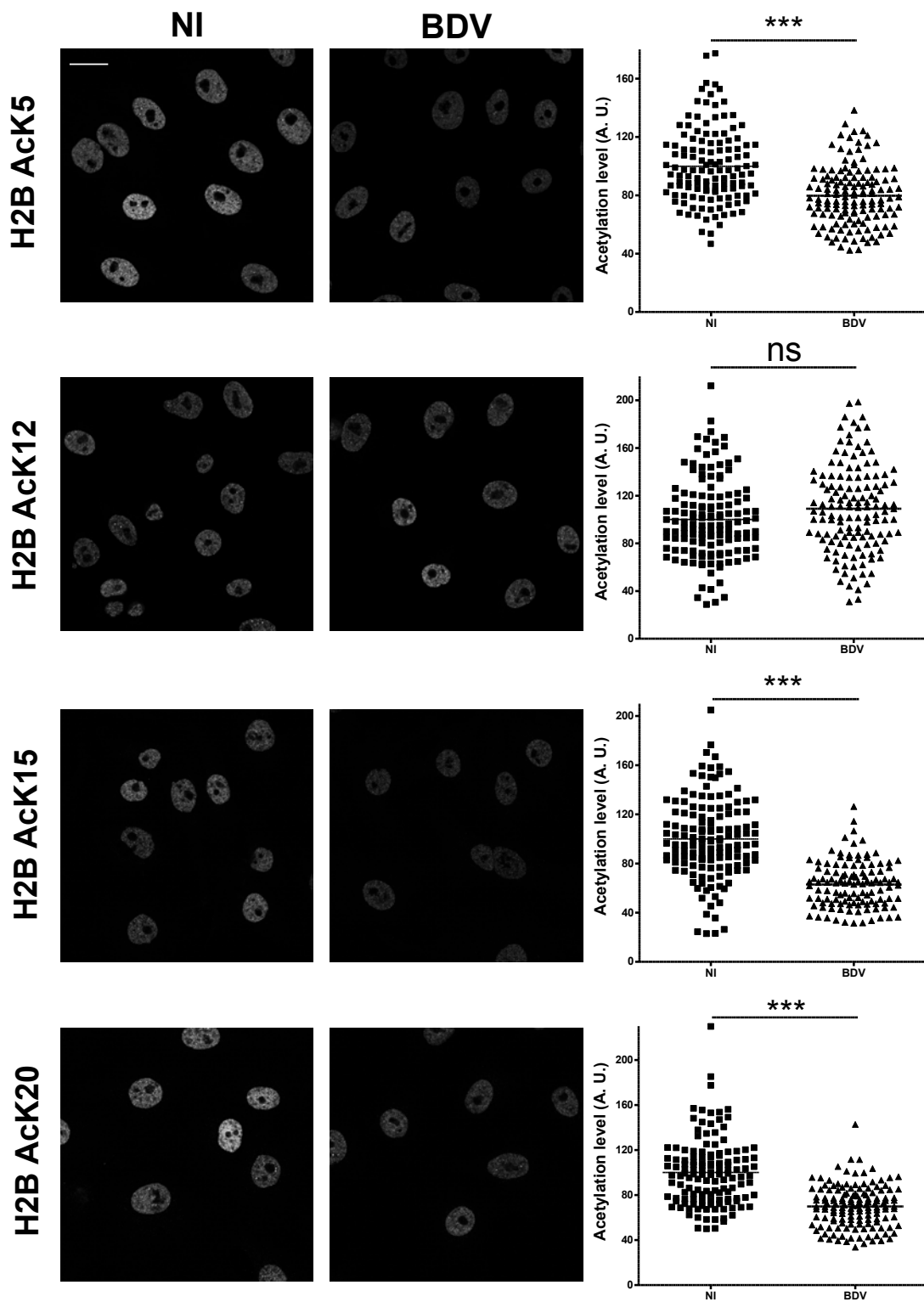
816



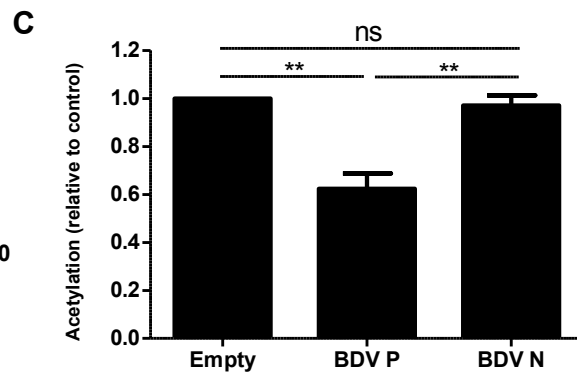
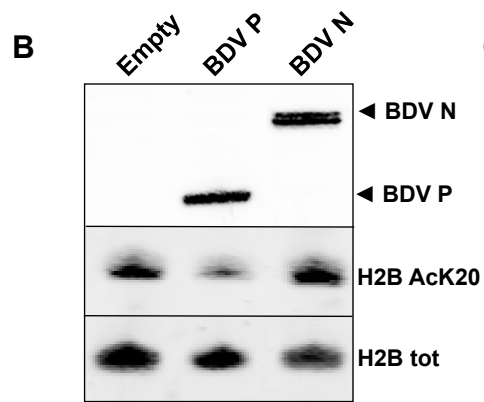
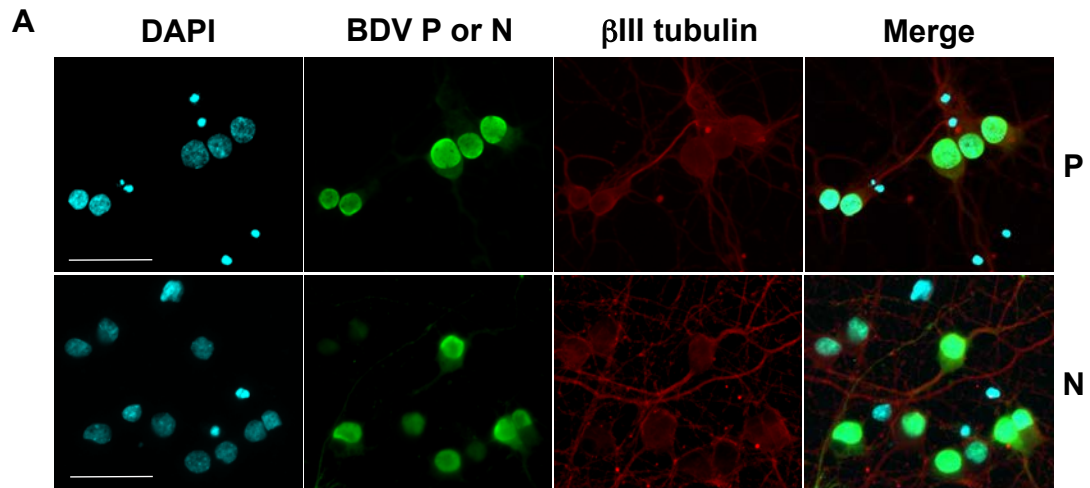
817
818



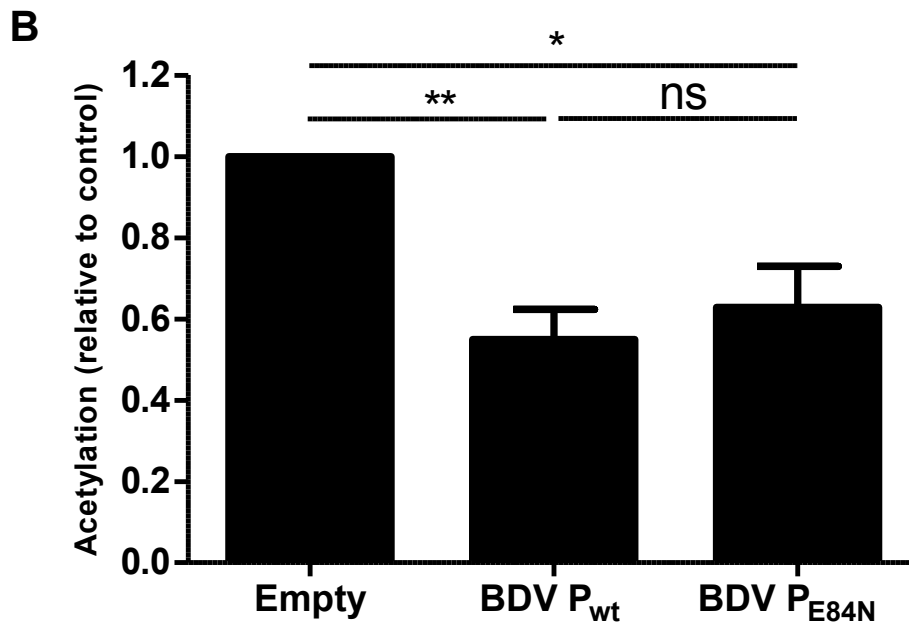
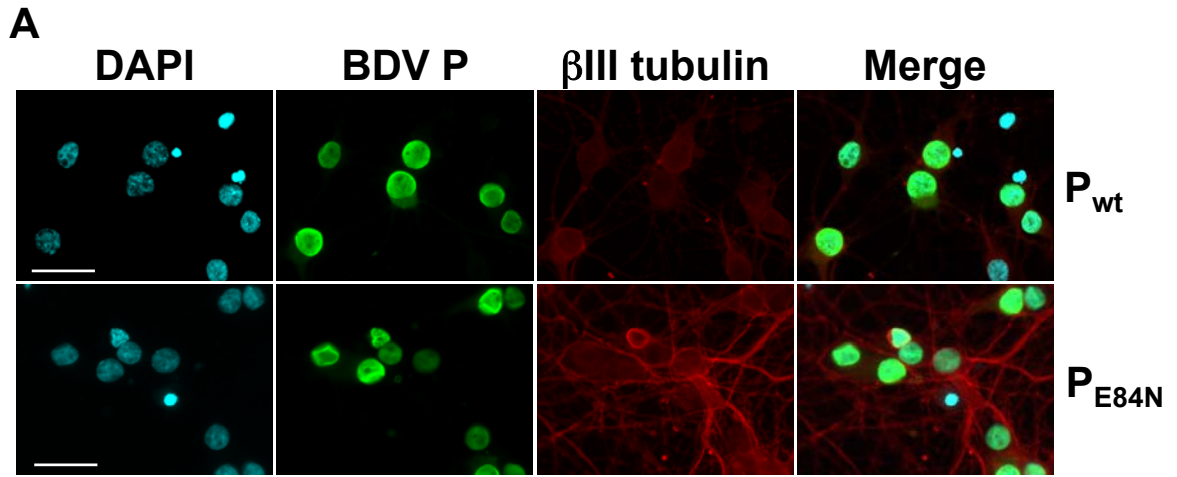
819
820

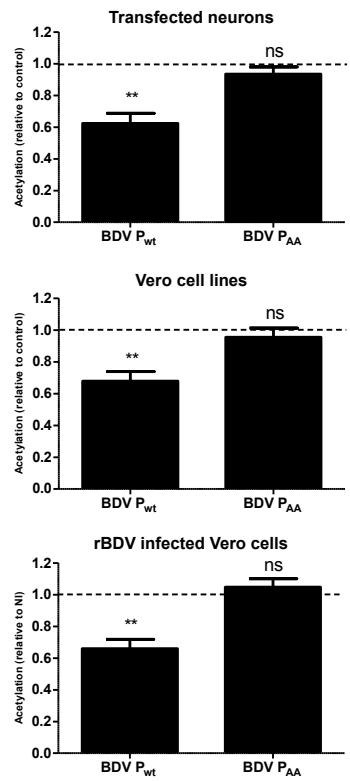
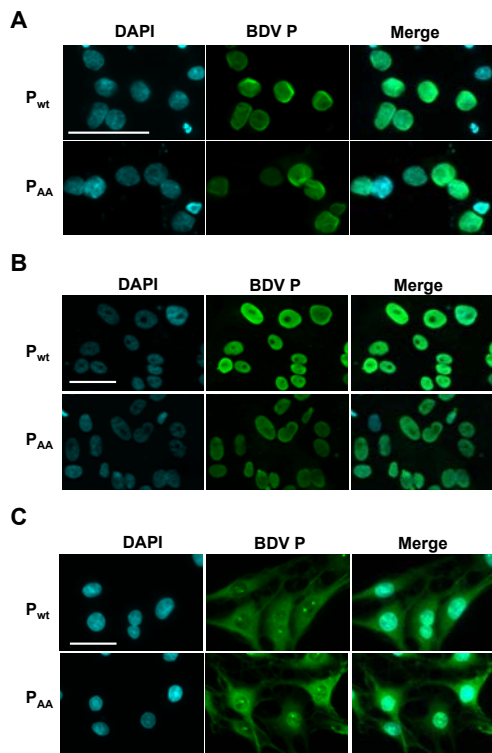


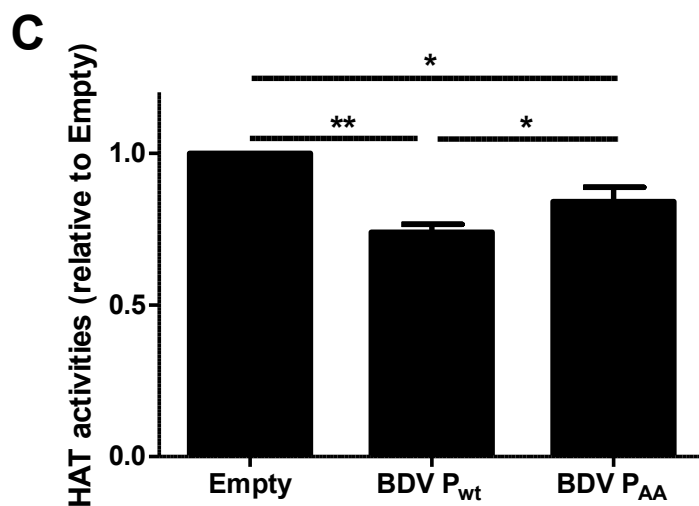
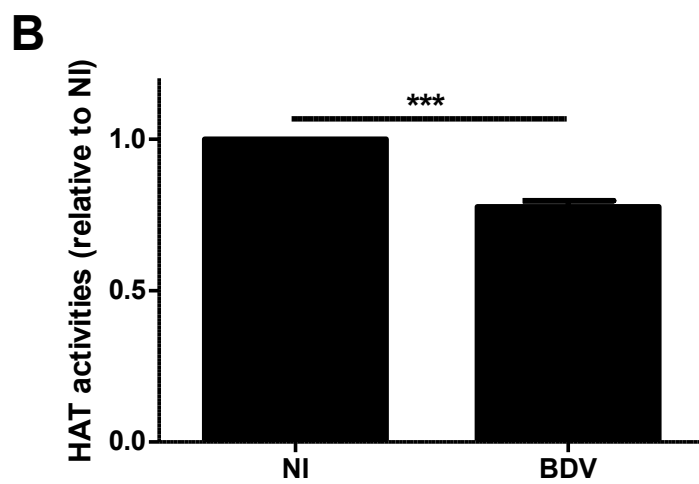
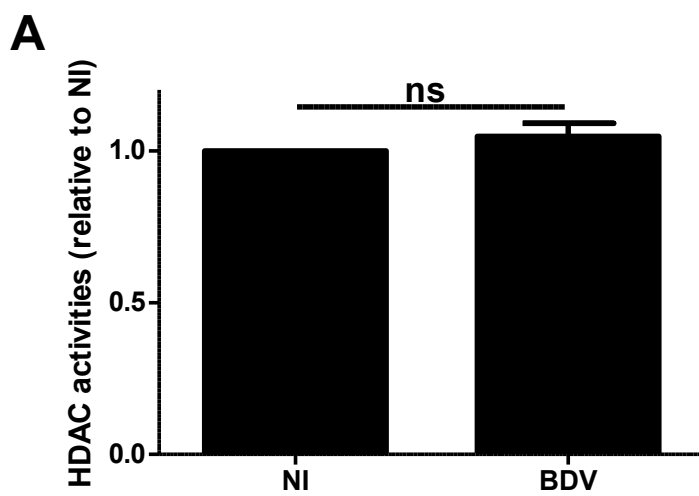
821

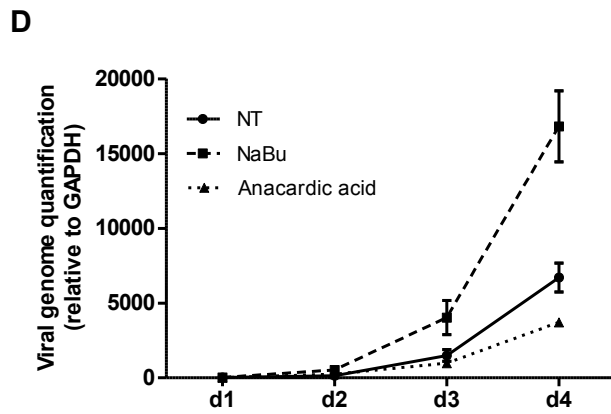
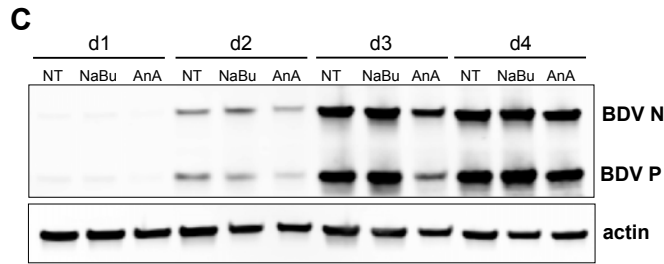
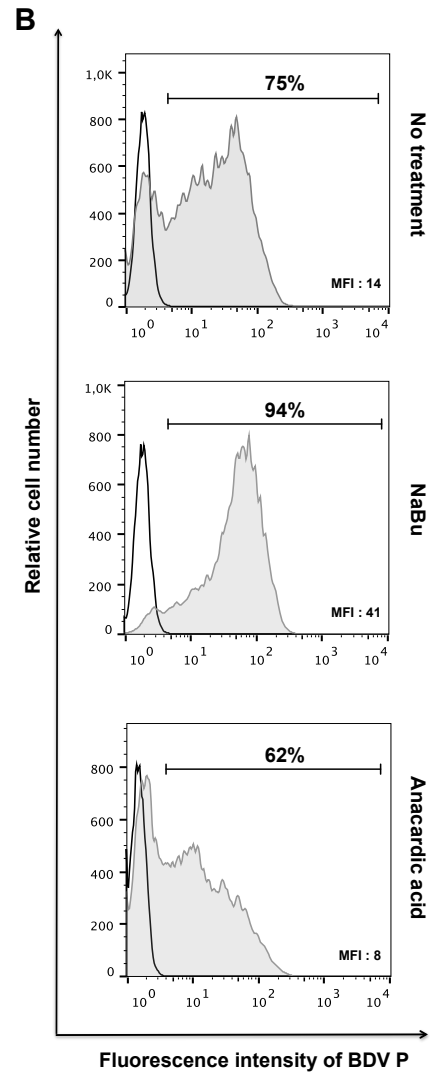
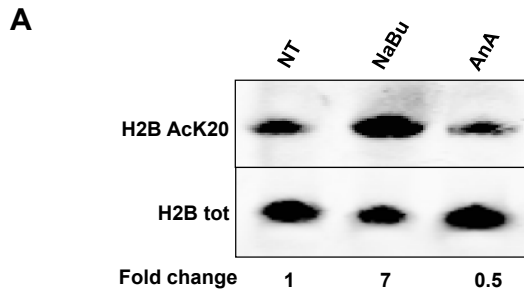


822

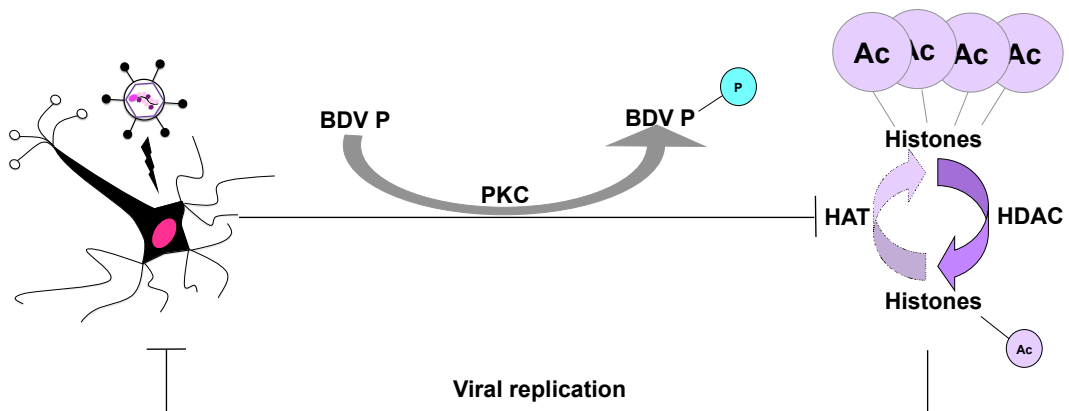








826
827



828